Multispectral labeling technique to map many neighboring axonal projections in the same tissue

Shlomo Tsuriel[1–4], Sagi Gudes[3,4], Ryan W Draft[1,2], Alexander M Binshtok[3,4] & Jeff W Lichtman[1,2]

We describe a method to map the location of axonal arbors of many individual neurons simultaneously via the spectral properties of retrogradely transported dye-labeled vesicles. We inject overlapping regions of an axon target area with three or more different colored retrograde tracers. On the basis of the combinations and intensities of the colors in the individual vesicles transported to neuronal somata, we calculate the projection sites of each neuron's axon. This neuronal positioning system (NPS) enables mapping of many axons in a simple automated way. In our experiments, NPS combined with spectral (Brainbow) labeling of the input to autonomic ganglion cells showed that the locations of ganglion cell projections to a mouse salivary gland related to the identities of their preganglionic axonal innervation. NPS could also delineate projections of many axons simultaneously in the mouse central nervous system.

Describing neuronal connectivity in detail is crucial for understanding how neuronal circuits work, but it is challenging because most neurons not only receive input from multiple sources distributed over a large portion of the nervous system but also send signals to target cells that are widely distributed. Progress has been made using retrograde trans-synaptic labeling approaches to identify the cohorts of neurons that are presynaptic to a given neuron[1,2]. Localizing all the postsynaptic targets of a neuron is more difficult. Most retrograde labeling techniques show all the neurons that project to a particular place but not all the places a neuron projects to. When multiple dyes are injected into different regions, the presence of doubly or triply colored retrogradely labeled cells shows that a neuron projects to two or three different regions[3–5]. However, these methods do not have enough resolution to show, for example, how much of an axon arbor is distributed to each of its target regions or how multiple neurons that project to the same regions differ in their projections. Therefore, the answer to the question of how the arbors of many different axons of the same class are organized relative to each other is largely unknown.

We have been interested in studying the organization of axonal projections among individual members of a single class of neurons. In a thin rodent muscle, the arbors of many overlapping neurons can be reconstructed by creating a high-resolution confocal montage of the entire set of arbors of all the axons and then reconstructing each[6]. But this approach does not scale well: as the number of axons being studied increases and the areal spread enlarges, the time to complete such a reconstruction becomes too long, and the sizes of the data sets become unmanageable.

Here we developed a multicolor retrograde labeling method, NPS, to define individual axonal arbors. This method does not require tracing out each branch of each axon and therefore scales well. To do this mapping we inject three to four differently colored probes into partially overlapping contiguous regions of a projection area and determine the spectral properties of each of many retrogradely transported vesicles in a cell body. We show that the color of each vesicle in the cell body maps to a site in the axon's projection.

In this study we first examined axonal projections in the mouse parasympathetic submandibular ganglion. The ganglion cell axons project into the submandibular gland, but little is known about their organization[7,8]. Using the NPS approach, we defined the axonal arborization area of individual ganglion cells and demonstrated that the projection territory of ganglion cell axons is linked to the particular presynaptic input each ganglion cell receives. Finally, we showed that the NPS approach can be used in the central nervous system (CNS) to map axonal projections between thalamus and cortex.

RESULTS

A method for mapping axonal projections of many neurons

To map the axonal output of many individual neurons in one specimen, we developed a labeling approach based on the spectral properties of retrogradely transported vesicles following injections of differently colored dyes in a target region. By analyzing the intensities and colors of individual retrogradely transported vesicles and matching those spectral properties to the distribution

[1]Center for Brain Science, Harvard University, Cambridge, Massachusetts, USA. [2]Department of Molecular and Cellular Biology, Harvard University, Cambridge, Massachusetts, USA. [3]Department of Medical Neurobiology, Institute for Medical Research Israel Canada Faculty of Medicine, The Hebrew University, Jerusalem, Israel. [4]The Edmond and Lily Safra Center for Brain Sciences, The Hebrew University, Jerusalem, Israel. Correspondence should be addressed to A.M.B. (alexander.binshtok@ekmd.huji.ac.il) or J.W.L. (jeff@mcb.harvard.edu).

RECEIVED 15 OCTOBER 2014; ACCEPTED 16 MARCH 2015; PUBLISHED ONLINE 27 APRIL 2015; DOI:10.1038/NMETH.3367

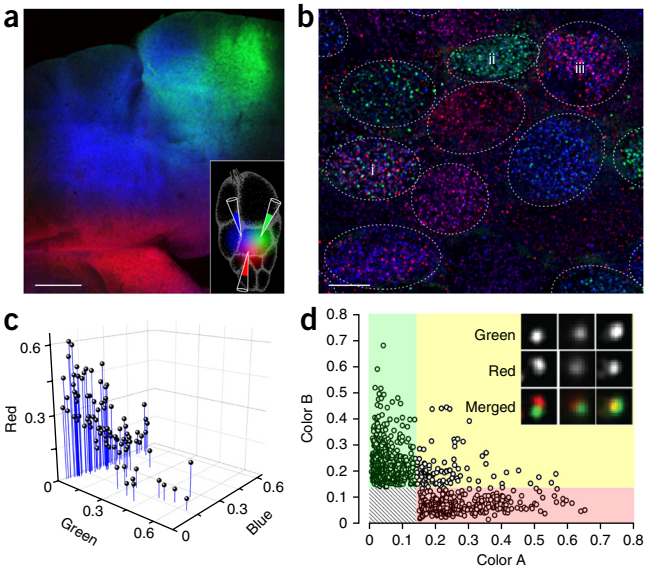

Figure 1 | Colors of retrogradely transported vesicles reflect a neuron's axonal projection. (**a**) In this one submandibular gland, we injected three differently colored WGA-conjugated fluorophores such that the red- and green-labeled territories do not overlap with each other but both overlap with the blue-labeled area. (**b**) About 16 h after the gland was labeled, clusters of submandibular ganglion cells imaged with confocal microscopy (~20 images per soma) exhibited a variety of differently colored vesicles but none that showed mixtures of red and green. Each dotted ellipse outlines a separate ganglion cell soma. (**c**) 3D scatter plot of the fluorescent intensity of vesicles in cell i in the three indicated channels (data from one representative cell out of six). Cell ii has only green and blue vesicles, and cell iii has only red and blue vesicles. (**d**) Vesicle intensities from six cells after two label injections into nonoverlapping regions of the gland. Two or three vesicles per cell (4.6%) appeared to have both of the colors (that were injected in nonoverlapping regions of the gland) above threshold. As shown in the inset, these 'vesicles' were superimpositions of vesicles that were located near each other (see **Supplementary Video 1**). Scale bars, 500 μm (**a**) and 10 μm (**b**).

of dyes in the target, we could construct the location of each neuron's axonal arbor.

We injected spectrally different Alexa Fluor (AF) fluorescent dyes conjugated to wheat germ agglutinin (WGA) to nearby locations in the submandibular salivary gland (**Fig. 1a**). Each of the dyes was injected in a single site within the gland and then diffused into surrounding regions. Because of the spread, different dyes overlapped at boundary areas between the injection sites (**Fig. 1a**). Between 16 and 20 h later we acquired high-resolution fluorescence confocal image stacks of submandibular ganglion cells that projected to the gland. These images revealed multiple labeled neuronal somata, and within each we observed fluorescently labeled vesicles (**Fig. 1b**). Given the colors, these vesicles must have been transported retrogradely from the injected areas of the gland. These vesicles varied in terms of both their intensities and color combinations even within single neurons (**Fig. 1b**,**c**).

We hypothesized that the reason for the color and intensity variability of the vesicles in a single cell is that vesicular uptake is local and reflects the dye combinations at the site of uptake. Given that an axon branches to several locations, the dye combinations should be different at each site. We further surmised that the vesicles remain separate from each other during transport to the soma and then at least for a time remain distinct in the soma. To test these ideas, we analyzed the transport of two dyes (red and green tagged WGA) that were injected into nonoverlapping regions of the gland. We found six ganglion cells that possessed both red- and green-labeled vesicles in their somata (**Fig. 1b**). 95.4% of the vesicles (372/390) had red or green fluorescence that was unmixed (either purely red or purely green), which is consistent with the idea that the dyes do not mix by fusion of vesicles during either transport or processing in the soma (**Fig. 1d** and **Supplementary Video 1**). The small percentage (4.6%) of vesicles that appeared to be both red and green were actually multiple vesicles that overlapped in the optical image as measured by the different center of gravity of the two colors (**Fig. 1d**). In contrast, when we injected a mixture of the colors to one site, the centers of gravity for the two colors in each vesicle were nearly identical. Thus, when axons extended into areas that had different colored dyes, the individual vesicles showed no mixing. These results imply that when a vesicle is filled with more than one color of dye it is because the dyes are present in the same region of the gland. This idea was confirmed by the blue dye injection that was also carried out in this same experiment. The blue dye overlapped with both the green and the red regions, and many vesicles contained both blue and green or both blue and red (**Fig. 1b**,**c**).

In addition to different color mixtures in the gland (that are reflected in different color mixtures in vesicles), the dye intensities varied throughout the gland owing to dilution according to the distance from the sites of dye injection. If the amount of

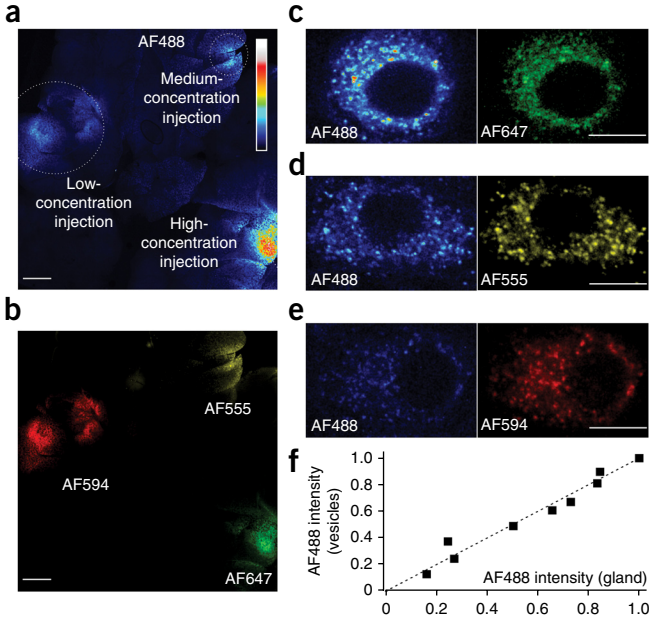

Figure 2 | The intensity of retrogradely labeled vesicles is a linear measure of the label intensity at axonal uptake sites. (**a**,**b**) Representative submandibular gland ($n = 4$) labeled with high, medium and low concentrations of WGA tagged with Alexa Fluor 488 (AF488) (**a**); these injections were premixed with WGA conjugated to three different fluorophores (**b**). (**c**–**e**) Left, different intensities of AF488 in ganglion cells from the three different injection sites confirmed by the highest-intensity labeling of any ganglion cells for each of the three co-mixed colors (right). (**f**) Comparison of the vesicle and gland dye intensity for 12 ganglion cells from 4 animals. Dashed line shows the optimal linear relation ($r = 0.98$). Scale bars, 500 μm (**a**,**b**) and 10 μm (**c**–**e**).

dye uptake by an axon into a vesicle is related to the concentration of the dye at the site of uptake, we would expect that some vesicles will be brighter than others. To test this idea we injected three regions of a gland with three different concentrations of WGA-AF488 (**Fig. 2a**) and co-injected a different color at each of these sites at high concentration to keep track of the vesicles' origins (**Fig. 2b–e**). We observed a linear relation between the dye intensity at injection sites and the dye intensity of vesicles that took up the dye from each of these sites (**Fig. 2f**). Moreover we saw no evidence of the presence of one color affecting the value of another color in the same vesicle. Therefore, we conclude that vesicle color-intensity combinations can be used to help determine the territory of a single axon branch. Moreover, documenting the color combinations in all the vesicles in a neuronal soma should reflect the spatial distribution of the entire projection of an axon within a dye-labeled area of the target tissue.

The mapping strategy is based on knowing the unique color combination and relative color intensities of dyes at each region of the injected gland. For example, if red, green and blue dyes are injected, axonal uptake from different regions will generate differently colored vesicles that mimic the color variations in the target tissue: a point in the gland near the blue injection site will have a high concentration of blue dye, a small concentration of red dye and an intermediate concentration of green dye. A different point might have more similar concentrations of the blue and red dye but a greater concentration of the green dye (**Fig. 3a**). When these matches are found for each vesicle, the projection of a neuron can be mapped automatically.

We used this retrograde labeling approach to map the axonal projections of many individual submandibular ganglion cell neurons that send their axons to the same gland target. We pressure-injected 0.5–1.5 µl of WGA tagged with four different spectrally distinct fluorophores (AF488, AF555, AF594 and AF647). The injections were made in four contiguous areas within the gland such that the concentrated WGA (10 mg ml^{-1}) at each injection site diffused into nearby areas and overlapped with the sites of dye spillover from other dye injections (**Fig. 3b**). In the experiments described below, the four dye injections covered an area of ~1 cm^2, or ~10% of the flattened gland surface.

We compared the color properties of 20–250 vesicles (mean ± s.e.m.: 78.8 ± 3.1) in each labeled neuron (**Fig. 3c**) with the dye distributions in the gland in order to locate the axonal projection of a neuron in the gland. This calculation is done in several steps. The first step is to assay the color intensities present in each vesicle in a neuron using a four-color confocal stack of images (in the case where four dyes are injected in the target). Second, for each color we normalize its intensities to the one vesicle in the entire set of ganglion cell clusters in an animal that exhibits the maximum intensity of that color. Drawing on the linear relationship between the dye intensity at injection sites and the dye intensity of vesicles (**Fig. 2f**), we assume that the vesicle in the whole set of ganglion cell clusters with the maximum intensity for one color (which we give an intensity of 1) must come from an axon branch at the site where the dye intensity in the gland is maximal. Third, we normalize the gland dye intensities to the sites of maximum intensity for each dye just as was done for intensities of vesicles in ganglia.

We use the four color values within each vesicle to find the site where the dye-injected gland best matches the vesicle's color intensities (**Fig. 3d**). In this way we map every vesicle to the site in the gland that most strongly correlates with its intensity profile. We then repeat the same procedure for all of the vesicles in a neuron to map the territory of its axonal arbor within the

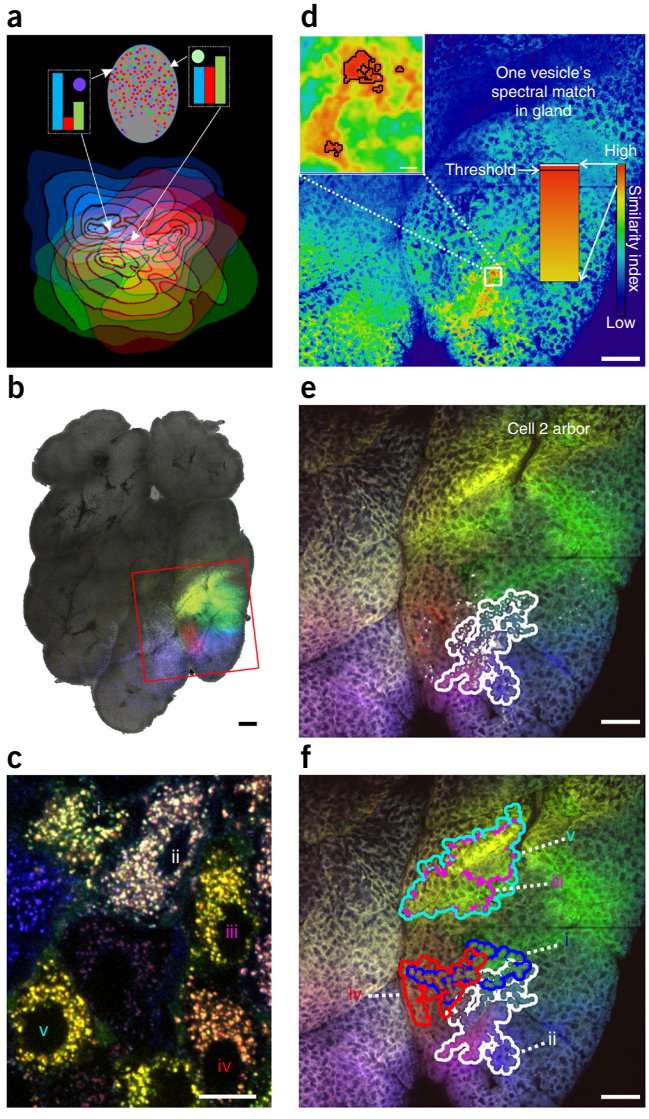

Figure 3 | A neural positioning system (NPS) for mapping axonal projections. (**a**) Diagram illustrating the rationale of the mapping technique. (**b**) Representative submandibular gland (of 50) showing the injection sites of WGA conjugated to four fluorophores (green, AF488; blue, AF555; red, AF594; yellow, AF647). Red rectangle marks the labeled area analyzed in **d–f**. (**c**) Ganglion cells that project to the dye-labeled gland region. (**d**) The mapping of one vesicle (from neuron ii in **c**) to the gland region is based on locating the pixels in the gland whose four color properties best match the color properties of the vesicle. Inset, magnified version of the gland volume denoted by the white box. The single pixel in the gland with the best match is shown in white in the inset. The regions bordered by a black outline are the pixels above the threshold. (**e**) Mapping all the vesicles of a neuron (cell ii in **c**). Each white dot represents the vesicle matches above the cutoff threshold. Shown is the outline of the contiguous region in the gland that best matched the range of colors of all the vesicles of neuron ii in **c**. (**f**) Analysis of the projections of cells i–v from **c**. Scale bars: 1 mm (**b**), 10 µm (**c**), 25 µm (**d** inset) and 500 µm (**d–f**).

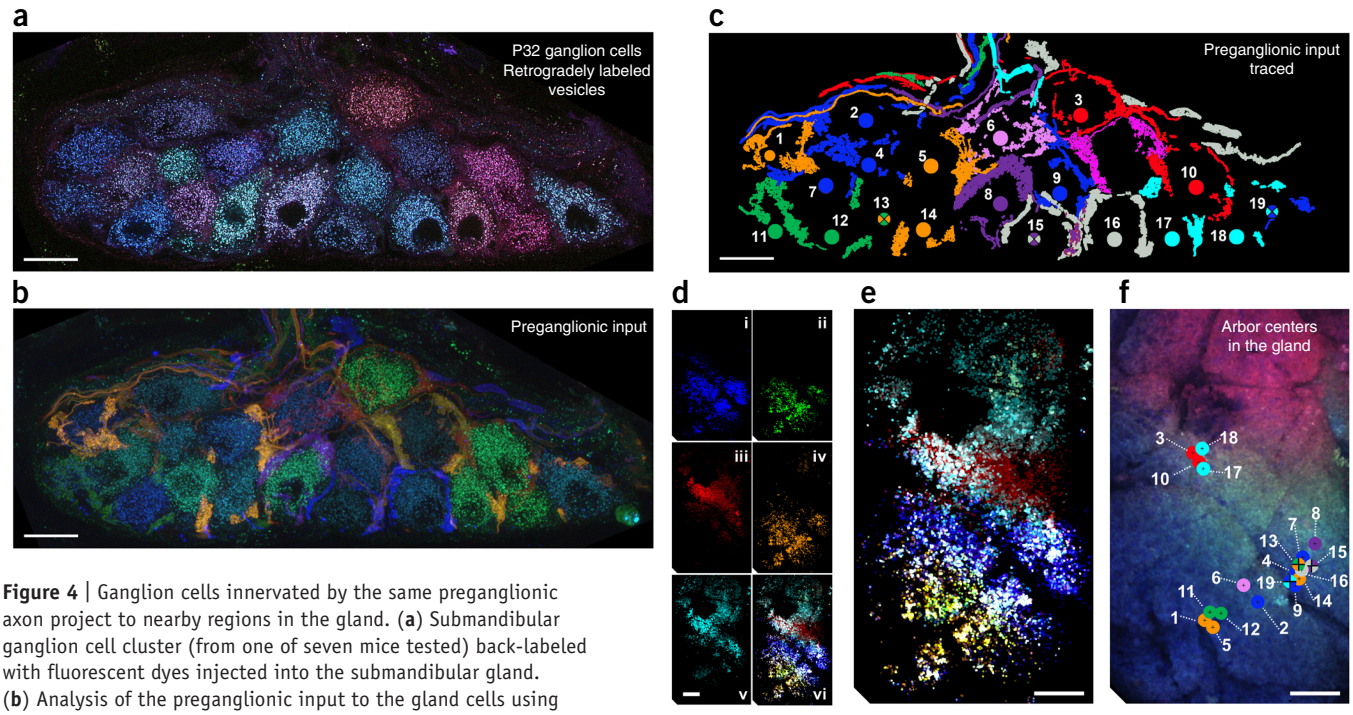

Figure 4 | Ganglion cells innervated by the same preganglionic axon project to nearby regions in the gland. (**a**) Submandibular ganglion cell cluster (from one of seven mice tested) back-labeled with fluorescent dyes injected into the submandibular gland. (**b**) Analysis of the preganglionic input to the gland cells using a Brainbow transgenic mouse line in which individual preganglionic axons are labeled with different combinations of three fluorescent proteins. The Brainbow labels and the AF-labeled retrograde vesicles can be distinguished by fluorescence intensity and location (Online Methods). (**c**) Rendering showing each of the preganglionic axons and the identity of each ganglion cell, based on data in **a** and **b**. The circle in each ganglion cell body represents the color of the preganglionic axon or axons that innervate it. (**d**) Projections of cohorts of ganglion cells based on the composite projections of all the neurons innervated by each of five different preganglionic axons. The superimposition of all these projections is shown in subpanel **vi**. (**e**) Higher-magnification image of **d**, **vi**. (**f**) Diagram showing the centers of gravity of the ganglion cell projections of each of the 19 cells shown in **a**–**c**. The color of each circle represents the identity of the innervating preganglionic axon. The locations are superimposed on the labeled gland image. Scale bars, 10 µm (**a**–**c**) and 500 µm (**d**–**f**).

gland (**Fig. 3e**). The composite result for all the vesicles in a ganglion cell generates a projection; this was usually 15–25 times larger than the area associated with a single vesicle. The territory occupied by a neuron was not usually homogeneous but clustered into a number of small areas, a pattern that was similar, both in size and organization, to the axonal arbors of transgenically labeled submandibular ganglion cells that terminate in multiple small 'baskets' (S. Sheu, J.C. Tapia and J.W.L., unpublished data). This similarity suggests that axons are collecting dye mostly from their terminal branches.

The analysis routine was accomplished by an automatic algorithm (see **Supplementary Software**) that allowed for analysis of multiple labeled ganglion cells in a cluster. As can be seen from this analysis, some neurons had nonoverlapping territories, but different neurons sometimes mapped to nearly identical regions (**Fig. 3f**).

In summary, our method assigns axonal arbor positions on the basis of the relation between vesicle color and the contours of the intensity profiles surrounding several differently colored injections in a target tissue. This strategy is in some ways analogous to the principle used in a Global Positioning System (GPS) receiver, which uses distances from three or more satellites to triangulate its position. For this reason we call our technique a neuronal positioning system (NPS).

Mapping two levels in the same synaptic circuit

To study the projections at two levels of a synaptic circuit in the peripheral nervous system, we applied the NPS method in Brainbow transgenic mice[9,10]. We have used a Thy1 membrane-tagged Brainbow construct (Mem-Brainbow) that labels nearly all of the preganglionic axons in a variety of different colors (**Fig. 4a**,**b**). Mem-Brainbow, however, is not expressed in ganglion cells, so the vesicle colors are not contaminated with Brainbow expression in ganglion cells. This approach allowed us to determine whether there was any relation between the axonal projections of postganglionic neurons and their upstream preganglionic innervation. In adult submandibular ganglia, preganglionic axons establish basket-like terminals on the somata of ganglion cells[7,11]. We studied the axonal projections via retrogradely labeled vesicles of ganglion cells in clusters of 20–80 neurons in young adult (postnatal day 32, or P32) Mem-Brainbow animals (**Fig. 4a**). Owing to Brainbow expression, we were also able to study the preganglionic input to these same cells (**Fig. 4b**,**c**). Ganglion cells that had the same preganglionic input appeared to project to the same area in the gland (**Fig. 4d**). For example, neurons 2, 4, 7 and 9 were all innervated by the 'blue' preganglionic axon (**Fig. 4c**) and all projected to neighboring areas (**Fig. 4d**, **i**). Superimposing the projections of the cohorts of ganglion neurons innervated by each preganglionic axon revealed a series of overlapping territories in the gland (**Fig. 4e**). We measured the distance between the centers of gravity of the axonal projections of pairs of ganglion cells that were innervated by the same preganglionic axon with pairs of ganglion cells innervated by different preganglionic axons. We found that each set of ganglion cells that was innervated by a single preganglionic axon tended to have its cells' projections clustered in a circumscribed part of the gland, and

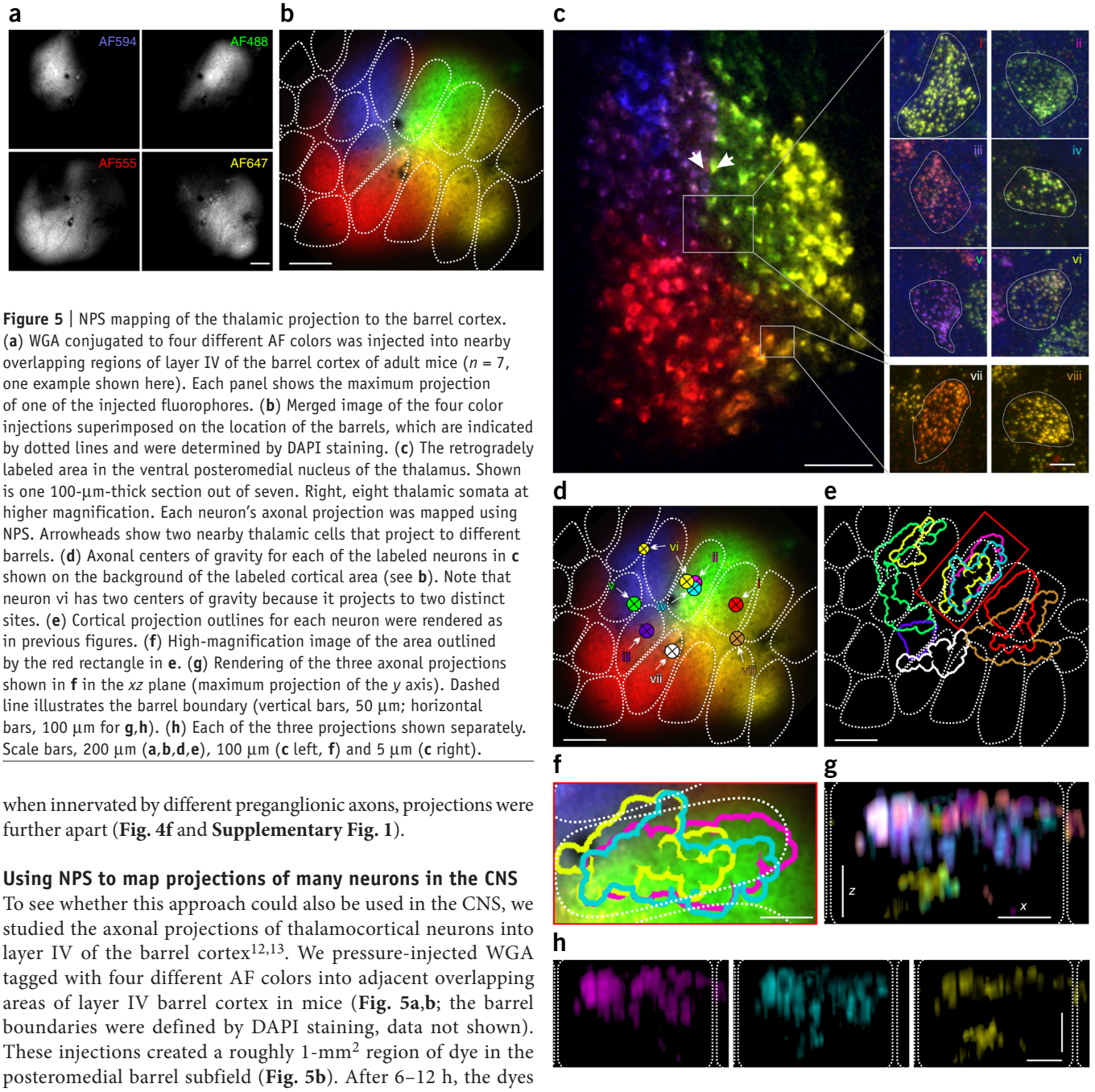

Figure 5 | NPS mapping of the thalamic projection to the barrel cortex. (**a**) WGA conjugated to four different AF colors was injected into nearby overlapping regions of layer IV of the barrel cortex of adult mice (n = 7, one example shown here). Each panel shows the maximum projection of one of the injected fluorophores. (**b**) Merged image of the four color injections superimposed on the location of the barrels, which are indicated by dotted lines and were determined by DAPI staining. (**c**) The retrogradely labeled area in the ventral posteromedial nucleus of the thalamus. Shown is one 100-µm-thick section out of seven. Right, eight thalamic somata at higher magnification. Each neuron's axonal projection was mapped using NPS. Arrowheads show two nearby thalamic cells that project to different barrels. (**d**) Axonal centers of gravity for each of the labeled neurons in **c** shown on the background of the labeled cortical area (see **b**). Note that neuron vi has two centers of gravity because it projects to two distinct sites. (**e**) Cortical projection outlines for each neuron were rendered as in previous figures. (**f**) High-magnification image of the area outlined by the red rectangle in **e**. (**g**) Rendering of the three axonal projections shown in **f** in the *xz* plane (maximum projection of the *y* axis). Dashed line illustrates the barrel boundary (vertical bars, 50 µm; horizontal bars, 100 µm for **g**,**h**). (**h**) Each of the three projections shown separately. Scale bars, 200 µm (**a**,**b**,**d**,**e**), 100 µm (**c** left, **f**) and 5 µm (**c** right).

when innervated by different preganglionic axons, projections were further apart (**Fig. 4f** and **Supplementary Fig. 1**).

Using NPS to map projections of many neurons in the CNS

To see whether this approach could also be used in the CNS, we studied the axonal projections of thalamocortical neurons into layer IV of the barrel cortex[12,13]. We pressure-injected WGA tagged with four different AF colors into adjacent overlapping areas of layer IV barrel cortex in mice (**Fig. 5a**,**b**; the barrel boundaries were defined by DAPI staining, data not shown). These injections created a roughly 1-mm^2 region of dye in the posteromedial barrel subfield (**Fig. 5b**). After 6–12 h, the dyes were visible in thalamic cell somata in the ventral posteromedial (VPM) nucleus (**Fig. 5c**). The thalamocortical neurons were labeled in a topographic manner that reflected the arrangement of dyes in the injected region of cortex (**Fig. 5b**,**c**). However, the color boundaries were often much sharper in the thalamus than in the cortex. For example, adjacent cells in one region were sharply partitioned into green and purple (**Fig. 5c**) with only a few cells sharing these colors, a result suggesting that the intervening sites in layer IV that contained the color mixture (green plus purple) were poorly innervated by thalamic axons from the examined area. This might be explained if axons from this thalamic area projected more often to barrels than to the septa between barrels (i.e., a barrelo-topic projection). Indeed, when we analyzed the projections of a set of thalamic neurons that fell at color boundaries, we found that most of them projected to barrels rather than septa. We analyzed 23–130 vesicles (mean ± s.e.m.: 50.1 ± 9.1, n = 13) per neuron (for example, **Fig. 5c**) and used NPS to map their neuronal projections to layer IV (**Fig. 5d**–**g**). The majority of the projections were within the borders of a single barrel (**Fig. 5d**,**e**). Some neurons had more than one projection area that covered more than one barrel, and some neurons projected more broadly to several barrels and in between them (**Fig. 5d**,**e**; see also ref. 14). NPS also delineated, in a given barrel, the projections of different neurons (**Fig. 5f**) in the horizontal and vertical planes, showing that these neurons projections largely overlapped in the horizontal plane but differed in which sublayers of layer IV that they projected to (**Fig. 5g**,**h**).

DISCUSSION

In this work we present an approach for mapping the axonal projections of each of many neurons in the same tissue at the same time. This technique should allow the mapping of all the neurons in a large area in a relatively easy way. The method relies on analysis of the colors of individual dye-labeled vesicles in the somata of neurons whose axons project to a target area that has been blanketed with gradients of several different colors of dyes. We used fluorescent conjugates of WGA because of its efficiency as a retrograde label[4,12,15]. It is likely that other retrogradely transported agents could also be used, but the WGA conjugates are relatively inexpensive and offer many color choices.

Because many neuronal somata could be studied in one tissue sample, this approach provided a means of mapping out the projections of many axons at the same time. To our knowledge there are no other techniques capable of this kind of detailed analysis of all the terminal branches of individual neurons in the same tissue sample.

We believe that large areas can be assessed with this approach. As shown in the salivary gland, the dye-filled target area was in the range of 1 cm^2. In the CNS, we injected an area that was about 1 mm^2, but this could have been much larger. The size of the dye-filled area can be increased by extending the distance between injection sites and increasing the injection volumes or by adding additional color channels (such as adding near-UV dye and blue dye channels, which were not used in the work we present here).

In conclusion, the ability to trace out the projections of many axons in the same piece of neural tissue offers an opportunity to learn about organizational principles that would otherwise be difficult or impossible to study. By seeing many axons in the same preparation, one can ascertain the way neurons in one region (and of one type) partition or mix relative to each other. Using this method in the parasympathetic nervous system, we found that axons that project to similar regions are innervated by the same presynaptic axon. This kind of interneuronal organization is probably commonplace in the nervous system but is invisible without methods to see each neuron as an individual entity rather than a member of a group of similarly labeled cells. Because this same labeling approach works well in the CNS, its use can potentially reveal how axonal projections are organized in many situations.

METHODS

Methods and any associated references are available in the online version of the paper.

Note: Any Supplementary Information and Source Data files are available in the online version of the paper.

ACKNOWLEDGMENTS

Support is gratefully acknowledged from the Humans Frontiers Science Foundation (S.T.), European Research Council (ERC) under the European Union's Seventh Framework Programme (FP7/2007-2013)/ERC grant agreement no. 260914 (S.T., S.G. and A.M.B.), US National Institute of Mental Health Silvio Conte Center 1P50MH094271 (J.W.L.) and US National Institutes of Health grant NS076467 (J.W.L.). We thank R. Kafri for helping generating the Matlab code.

AUTHOR CONTRIBUTIONS

S.T. conceived of the NPS strategy, designed and conducted the experiments, analyzed the data and wrote the manuscript. S.G. conducted the experiments, analyzed the data and wrote the manuscript. R.W.D. created Mem-Brainbow mice and wrote the manuscript. A.M.B. designed the experiments, analyzed the data, supervised the project and wrote the manuscript. J.W.L. conceived of the study, designed the experiments, analyzed the data, supervised the project and wrote the manuscript.

COMPETING FINANCIAL INTERESTS

The authors declare no competing financial interests.

1. Wickersham, I.R., Finke, S., Conzelmann, K.-K. & Callaway, E.M. Retrograde neuronal tracing with a deletion-mutant rabies virus. *Nat. Methods* **4**, 47–49 (2007).
2. Wickersham, I.R. *et al.* Monosynaptic restriction of transsynaptic tracing from single, genetically targeted neurons. *Neuron* **53**, 639–647 (2007).
3. Bentivoglio, M. & Molinari, M. Fluorescent retrograde triple labeling of brainstem reticular neurons. *Neurosci. Lett.* **46**, 121–126 (1984).
4. Reeber, S.L., Gebre, S.A. & Sillitoe, R.V. Fluorescence mapping of afferent topography in three dimensions. *Brain Struct. Funct.* **216**, 159–169 (2011).
5. Sincich, L.C., Jocson, C.M. & Horton, J.C. V1 interpatch projections to V2 thick stripes and pale stripes. *J. Neurosci.* **30**, 6963–6974 (2010).
6. Lu, J., Tapia, J.C., White, O.L. & Lichtman, J.W. The interscutularis muscle connectome. *PLoS Biol.* **7**, e32 (2009).
7. Lichtman, J.W. The reorganization of synaptic connexions in the rat submandibular ganglion during post-natal development. *J. Physiol. (Lond.)* **273**, 155–177 (1977).
8. Snider, W.D. The dendritic complexity and innervation of submandibular neurons in five species of mammals. *J. Neurosci.* **7**, 1760–1768 (1987).
9. Livet, J. *et al.* Transgenic strategies for combinatorial expression of fluorescent proteins in the nervous system. *Nature* **450**, 56–62 (2007).
10. Cai, D., Cohen, K.B., Luo, T., Lichtman, J.W. & Sanes, J.R. Improved tools for the Brainbow toolbox. *Nat. Methods* **10**, 540–547 (2013).
11. McCann, C.M., Tapia, J.C., Kim, H., Coggan, J.S. & Lichtman, J.W. Rapid and modifiable neurotransmitter receptor dynamics at a neuronal synapse *in vivo*. *Nat. Neurosci.* **11**, 807–815 (2008).
12. Gonatas, N.K., Harper, C., Mizutani, T. & Gonatas, J.O. Superior sensitivity of conjugates of horseradish peroxidase with wheat germ agglutinin for studies of retrograde axonal transport. *J. Histochem. Cytochem.* **27**, 728–734 (1979).
13. Wan, X.C., Trojanowski, J.Q. & Gonatas, J.O. Cholera toxin and wheat germ agglutinin conjugates as neuroanatomical probes: their uptake and clearance, transganglionic and retrograde transport and sensitivity. *Brain Res.* **243**, 215–224 (1982).
14. Oberlaender, M. *et al.* Cell type-specific three-dimensional structure of thalamocortical circuits in a column of rat vibrissal cortex. *Cereb. Cortex* **22**, 2375–2391 (2012).
15. Zhong, F., Christianson, J.A., Davis, B.M. & Bielefeldt, K. Dichotomizing axons in spinal and vagal afferents of the mouse stomach. *Dig. Dis. Sci.* **53**, 194–203 (2008).

ONLINE METHODS

Animals and labeling. All animal experiments were approved by the Faculty of Arts and Sciences Institutional Animal Care and Use Committee of Harvard University or the Ethics committee of Hebrew University. Male and female C57 black mice were anesthetized with 100 mg per kg body weight (mg kg^{-1}) ketamine and 10 mg kg^{-1} xylazine. The ventral neck hair was then removed (using a commercial hair removal cream), and a 1- to 3-cm midline incision was made from the base of the chin to the sternum to expose the submandibular glands bilaterally. To inject the gland(s) with dyes, we used a pulled glass pipette attached to a syringe. The injections were done in the lateral lower third of one or both glands by applying hand pressure to a syringe after inserting the pipette several tens of micrometers beneath the gland capsule. At each injection site, ~0.5 µl of 10 mg ml^{-1} wheat germ agglutinin (WGA) conjugated to Alexa Fluor (AF, Invitrogen) 488, 555, 594 or 647 was injected. In principle, to localize a point on a two-dimensional (2D) surface, three colors are sufficient, and for mapping a 3D space, no more than four colors are needed. Although the salivary gland is 3D, we restricted the injections to regions near the gland's surface where imaging the dye concentrations is more straightforward owing to less scatter. The areas that we studied were restricted to a 150-µm rind near the gland surface, and we kept track of the *x*, *y* and *z* coordinates of the dye spread. We found as expected that when we ignored all but one color, the positioning result of each vesicle degraded. The precision of vesicle mapping to the gland improved progressively with each additional color channel up to the four we tried (data not shown).

The injections within each gland were spaced ~1 mm apart from each other in a square-shaped pattern. After the injections, the ventral skin was sutured, and the was animal monitored until surgical recovery and provided with an injection of buprenorphine (0.1 mg kg^{-1}) for pain management. Because vesicles that are transported back to the soma eventually enter larger organelles in the lysosomal pathway and get degraded (at ~1 week after dye injection there is no color in the ganglion cell somata), we did all imaging between 16 and 20 h after target injection, when the vesicles had just appeared in the ganglion cell somata and well before the lysosomal process had removed them. The animals were reanesthetized and perfused transcardially with cold (4 °C) fixative solution containing 4% paraformaldehyde and 120 mM sucrose in PBS. The gland, ganglion tissue and duct were then extirpated. To prepare for histological study, we pressed the gland between two glass slides in fixative solution for 3 h. The duct was incubated for 1 h in fixative solution and for another 1 h in fixative solution with 1% Triton X-100.

A subset of the mice used in this study also expressed a Brainbow transgene (Mem-Brainbow), resulting in fluorescent labeling of ~90% of preganglionic axons that project to the submandibular ganglion. To make this transgenic line, we first cloned a CMV-Brainbow 1.0–style construct using membrane-bound fluorescent proteins and pairs of incompatible *loxP* and *lox2272* sites (as described in ref. 9). The construct encodes (5′ to 3′) mCherry[16], monomeric EYFP (ref. 17) and monomeric Cerulean[18]. A short palmitoylation sequence[19] was fused to a linker at the N terminus of each protein. The Thy1 Mem-Brainbow construct was generated by blunt-cloning a Nhe1/Sca1 fragment containing the Brainbow coding region (3.4 kb) into the Xho1 site of the Thy1.2 cassette[20]. Mem-Brainbow mice were crossed with a Thy1-Cre transgenic line[21] to switch expression from default mCherry to Cerulean or EYFP.

Injection to the barrel cortex. We stereotactically injected WGA conjugated to AF dye 488, 555, 594 or 647 into layer IV of the primary somatosensory barrel cortex of 6- to 8-week-old C57BL/6 mice, using pulled glass pipettes attached to a syringe. Injections were carried out under isoflurane anesthesia (2%). Anesthetized mice were placed in a stereotaxic frame (David Kopf instruments) and maintained on a heating blanket at 37 °C. The animals' heads were shaved, and a midline incision was made in the scalp to identify the bregma and the lambda. The location of the barrel cortex and the injection sites were estimated using the known stereotaxic coordinates[22] (for mice with 4.1 bregma-lambda distance as follows: −0.8 mm AP from the bregma; 3.1 mm lateral from the bregma; 0.56 mm ventral to the skull surface). Bregma-lambda distance was measured in each animal, and adjustments were made accordingly. Using a small dental drill to allow for pipette insertion, we drilled four holes 100 µm posterior, anterior, medial and lateral to the above coordinates. Approximately 20 nl of each dye were injected into each hole. The injection pipette was left at each injection site for 10 min. After the injections, the skin was sutured and the animal monitored until it woke, at which point it was provided with an injection of buprenorphine (0.1 mg kg^{-1}) for pain management. Six to eight hours after the injections, the mice were reanesthetized and perfused transcardially with 20 ml PBS followed by 15 ml of 4% PFA. Brains were removed and post-fixed in 4% PFA at 4 °C for 6 h and then mounted in 1% agarose. A single slice containing layer IV of somatosensory cortex was obtained by precutting the brains in the tangential plane as previously described[23,24]. In brief, this was accomplished by trimming the base of the brain at a 30° angle relative to the horizontal plane and at a 10° angle relative to the vertical plane. The block was then oriented in a microtome (Leica V1000) with the trimmed surface down, so that the plane of the knife was tangential to the pial surface of the barrel field. The first 200-µm slice, which contained layers I and II and most of layer III, was discarded. The subsequent 400-µm slice, in which the posteromedial barrel subfield was clearly visible using 4,6-diamidino-2-phenylindole (DAPI) staining, was taken for the analysis. The remaining brain block was sliced coronally in 100-µm sections, and the ventral posteromedial (VPM) nucleus and posteromedial complex (PoM) of thalamus were identified using mouse brain maps[22].

Sample size and blinding. For the vesicle mixing test (**Fig. 1**), 18 animals were injected and scanned in attempt to find two dyes that do not overlap in the gland but have ganglion cells with both colors. This was found in only one animal, in which 390 vesicles in six cells were analyzed.

For intensity comparisons (**Fig. 2**), we used four animals (three maximal-intensity vesicles in each animal were tested to generate the correlation plot (**Fig. 2f**)).

For measurements of distances between axonal arbors (**Fig. 4** and **Supplementary Fig. 1**), we used three animals of P32 and four animals of P18. We analyzed one ganglion in each animal with a total of 56 neurons in P32 and 59 neurons in P18.

For the CNS labeling (**Fig. 5**), seven animals were used, for which one representative animal is shown.

We did not carry out a power analysis because this is a new approach and we had no way to estimate the effect size. We took and analyzed all the data using a minimum of three animals. In all experiments, the detection of vesicles was performed blindly with respect to the vesicle's original color. In the Brainbow experiments (**Fig. 4** and **Supplementary Fig. 1**), detection of preganglionic colors was performed blindly with respect to the ganglionic arbor analysis.

No randomization was used.

Imaging equipment and settings. The target tissue was imaged on a laser scanning confocal (Zeiss LSM 7 or Leica SP5) using a 10×, 0.3–numerical aperture (NA) air objective at 2.8 × 2.8 × 5 μm^3/voxel in the gland and 1.5 × 1.5 × 4 μm^3/voxel in the barrel cortex. Retrogradely labeled ganglia of thalamus were imaged with a 63×, 1.4-NA oil objective at 0.09 × 0.09 × 0.4 μm^3/voxel. We used a 488-nm argon laser to excite AF488 (490- to 523-nm emission); a 561-nm photodiode laser (562- to 584-nm emission) was used for AF555; a 594-nm photodiode laser (597- to 632-nm emission) for AF594; and a 633-nm photodiode laser (659- to 740-nm emission) for AF647. The Brainbow labels are less intense than the AF-labeled vesicles so that the gain can be turned down to the point where only the vesicles are visible (for example, **Fig. 4a**). For these reasons and the different localization of preganglionic axons that surround ganglion cells versus the intracellular vesicle labeling of ganglion cells *per se*, it was possible to disambiguate the preganglionic colors from the ganglion cell vesicle colors (**Fig. 4b**). To image the Brainbow colors in the preganglionic axons, we used a 440-nm photodiode laser (459-to 487-nm emission) for CFP and a 514-nm argon laser (516- to 544-nm emission) for EYFP. To enhance the intensity of mCherry, we used a previously described custom rabbit anti-mCherry antibody[13] (1:1,000) that was bound to a secondary anti-rabbit antibody coupled to AF633. For imaging AF633, we used a 633-nm photodiode laser (640- to 694-nm emission). Each channel was imaged sequentially. WGA-AF fluorescence was much brighter than the intrinsic XFP Brainbow fluorescence. Although the Brainbow and the AF channels overlap, they are distinguishable by their different location (preganglionic axons surrounding ganglion cell bodies versus retrogradely vesicles inside the ganglion cell body).

Image analysis. NPS analyses, as executed in this paper, are based on the assumption that for each dye the sites of maximal dye concentration in the target area are in fact innervated by at least some neurons in the presynaptic population.

In order to reduce noise we used a two-pixel radius Gaussian filter on the target confocal images and a one-pixel radius filter on the ganglion or thalamus. Each analyzed soma was separated into a 3D cube that contained most of its retrogradely transported vesicles (>90%) and, more importantly, contained no vesicles from any other cell as these would contaminate the interpretation. To get the location of each vesicle, we used the brightest pixel value among the four color channels of the ganglion somata images. These brightest values were merged into one 3D image that contain only the maximal values from all channels for each pixel in each image of the stack. We used the ImageJ 3dobject counter plug-in[25] to threshold the vesicles and localize them in 3D space. We excluded fluorescent spots that were noise because they were smaller than the diffraction limit (occupied less than ten voxels, 0.039 μm^3) or larger than the diffraction limit (50 voxels = 0.19 μm^3 as more than one vesicle).

Using the coordinates that localized the vesicles (see above), we then obtain the maximal value from each channel for each vesicle. Next, these values are normalized to the brightest vesicle value in the entire ganglion for each color channel. Using a custom Matlab script (see **Supplementary Software**) we studied each vesicle sequentially by comparing its normalized value in each of the four color channels to the normalized values of the color channels at every position in the gland. The comparison was accomplished by generating a difference value for each vesicle color with each gland pixel. These four differences were then summed for each gland pixel:

$$|V_{\text{green}} - G_{\text{green}N}| + |V_{\text{yellow}} - G_{\text{yellow}N}| + |V_{\text{orange}} - G_{\text{orange}N}| + |V_{\text{red}} - G_{\text{red}N}|$$

Where V is the normalized vesicle value for a color channel; green, yellow, orange and red are the different channels. G is the normalized gland value for a color channel at pixel N.

The pixel in the gland with the minimal sum of the differences is the pixel whose composite four-color distribution best matches that vesicle's four-color distribution (i.e., the best fit). In order to reduce noise for each vesicle, we marked the 0.0001% of best-fit pixels as the possible origin for the vesicle. In most cases these gland pixels were localized to the same area in the gland. To create the locale of the axonal projection of a single ganglion cell, we drew the perimeter surrounding the best-fit pixels for all of the vesicles in the ganglion cell and circling 10- to 15-pixel radius around each that typically generated one or at most several contiguous regions.

To quantitate the size of these arbors, we use a measure of arbor length that is the distance between the two most geometrically distant points in the arbor. Arbor area and length were calculated on a 2D image that was created by summing best-fitted points from the 3D image. We also calculated the arbor center of gravity using a Matlab script that averaged the coordinates of all the fit pixels in the x, y and z axes. The center of gravity was used to calculate the distances between pairs of neuron's arbors.

Statistics. For all statistical comparisons we used the unpaired one- and two-sided student t-test corrected for the multiple comparisons, and one way ANOVA, $^*P < 0.05$, $^{**}P < 0.01$, $^{***}P < 0.001$, with *post hoc* Bonferroni correction. Data are represented as mean ± s.e.m. F-tests were used to examine the similarity of the variance of the compared groups, and the appropriate t-tests were performed accordingly.

16. Shaner, N.C. *et al.* Improved monomeric red, orange and yellow fluorescent proteins derived from Discosoma sp. red fluorescent protein. *Nat. Biotechnol.* **22**, 1567–1572 (2004).
17. Zacharias, D.A., Violin, J.D., Newton, A.C. & Tsien, R.Y. Partitioning of lipid-modified monomeric GFPs into membrane microdomains of live cells. *Science* **296**, 913–916 (2002).
18. Rizzo, M.A., Springer, G.H., Granada, B. & Piston, D.W. An improved cyan fluorescent protein variant useful for FRET. *Nat. Biotechnol.* **22**, 445–449 (2004).
19. Kay, J.N. *et al.* Transient requirement for ganglion cells during assembly of retinal synaptic layers. *Development* **131**, 1331–1342 (2004).

doi:10.1038/nmeth.3367

20. Caroni, P. Overexpression of growth-associated proteins in the neurons of adult transgenic mice. *J. Neurosci. Methods* **71**, 3–9 (1997).
21. Dewachter, I. *et al.* Neuronal deficiency of presenilin 1 inhibits amyloid plaque formation and corrects hippocampal long-term potentiation but not a cognitive defect of amyloid precursor protein [V717I] transgenic mice. *J. Neurosci.* **22**, 3445–3453 (2002).
22. Paxinos, G. & Franklin, K.B.J. *The Mouse Brain in Stereotaxic Coordinates* 2nd edn. (Academic Press, 2004).
23. Binshtok, A.M., Fleidervish, I.A., Sprengel, R. & Gutnick, M.J. NMDA receptors in layer 4 spiny stellate cells of the mouse barrel cortex contain the NR2C subunit. *J. Neurosci.* **26**, 708–715 (2006).
24. Fleidervish, I.A., Binshtok, A.M. & Gutnick, M.J. Functionally distinct NMDA receptors mediate horizontal connectivity within layer 4 of mouse barrel cortex. *Neuron* **21**, 1055–1065 (1998).
25. Bolte, S. & Cordelières, F.P. A guided tour into subcellular colocalization analysis in light microscopy. *J. Microsc.* **224**, 213–232 (2006).